ChemComm

Tuning the Allosteric Sequestration of Anticancer Drugs for Developing Cooperative Nano-Antidotes

Journal:	*ChemComm*
Manuscript ID	CC-COM-12-2019-009373.R1
Article Type:	Communication

COMMUNICATION

Tuning the Allosteric Sequestration of Anticancer Drugs for Developing Cooperative Nano-Antidotes

Received 00th January 20xx,
Accepted 00th January 20xx

DOI: 10.1039/x0xx00000x

Weikun Wang,[a] Tyler J. Finnegan,[a] Zhiquan Lei,[a] Xingrong Zhu,[a] Curtis E. Moore,[a] Kejia Shi[a] and Jovica D. Badjić*[a]

Dual-cavity basket 1^{6-}, holding six γ-aminobutyric acids at its termini, encapsulates variously sized aromatics 2–7^+, including four anthracyclines (8^+–11^+), driven by the hydrophobic effect and hydrogen bonding (HB). In particular, the formation of stable (K = 10^{12} M^{-2}) anthracycline complexes [(8^+–11^+)$_2$⊂1^{6-}]], assembled into nanoparticles, occurred with positive homotropic cooperativity (α = $4K_2/K_1$ = 1.1 ± 0.3 · 10^2 − 1.3 ± 0.7 · 10^3) in PBS medium. Importantly, weakening the first binding event (K_1, *i.e.* by removing HBs) turned the second one (K_2) more favorable. The concept is of interest for developing cooperative nano-antidotes acting as biodetoxifying agents.

With regard to pharmacological strategies[1] for relieving the effects of illicit drug consumption,[2] suicide attempts,[3] and accidental exposure[4] to toxic materials, there is immediate need for developing new antidotes.[5] So far, detoxifying agents (a) act as antagonists and occupy the binding sites of biological receptors (i.e. naloxone, atropine)[6] or (b) reduce the concentration of toxicants in blood by either promoting their rapid degradation or removal via encapsulation.[7] Indeed, the later so-called pharmacokinetic (PK) strategy[8] has been explored with enzymes,[9] antibodies[10] and abiotic hosts[11] of which the development of γ-cyclodextrin derivative sugammadex[12] steals the spotlight. In brief, sugammadex is capable of complexing (K_a = 10^7 M^{-1}) muscle relaxants rocuronium and vecuronium used in anaesthesia to eliminate their physiological effects during postoperative care and recovery.[13] In this respect, we recently reported[14] about the capacity of basket $\mathbf{1}^{6-}$ (Figure 1A) for holding anticancer drug doxorubicin (DOX, Figure 1B) in its two cavities. The dual-cavity host acted in an allosteric manner[15] with the first complexation greatly facilitating the second one (α = $4K_2/K_1$ = 1.1 ± 0.3 · 10^2 and $K_1 \cdot K_2$=10^{12} M^{-2}).[16] The formation of ternary [$\mathbf{DOX}_2$⊂$\mathbf{1}^{6-}$] was also accompanied by their assembly into stable spherical

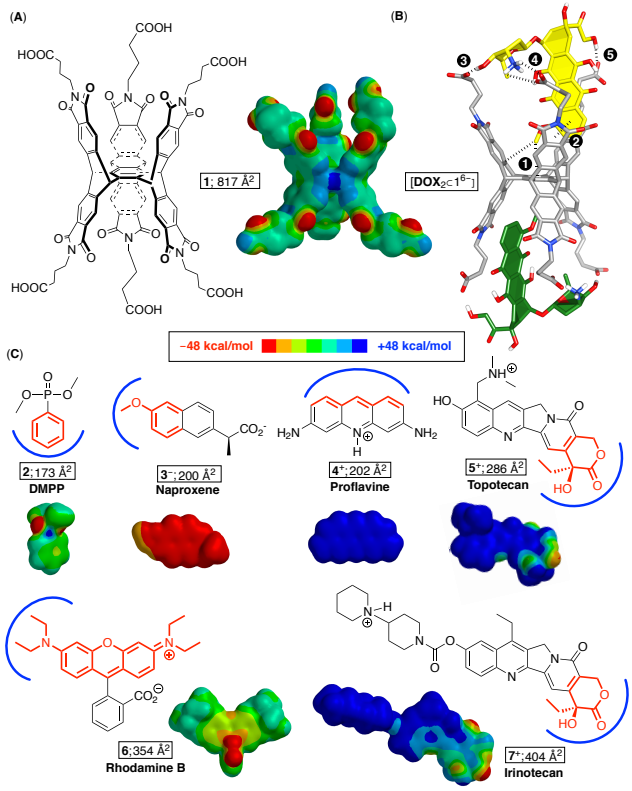

Figure 1. (A) Chemical structure of dual-cavity basket **1** along with its EPS (PM3, Spartan) and the computed solvent-accessible surface area (SASA; PM3, Spartan). (B) A working model of energy-minimized [$\mathbf{DOX}_2$⊂$\mathbf{1}^{6-}$] (MM/MC, OPLS3) showing **1**–**5** intermolecular contacts. (C) Chemical structures and computed EPSs/SASAs (PM3, Spartan) of guests **2**–$\mathbf{7}^+$. The red colored region of each molecule denotes its portion embedded in the basket's cavity as deduced from ^{1}H NMR spectroscopic measurements.

nanoparticles (circa 50 nm).[17] From the results of computational studies,[14] we hypothesized that the positive homotropic cooperativity[18] emerged from an induced-fit mode of action[19] in which, we posited, hydrophobic effect and directional drug-to-basket noncovalent contacts (hydrogen bonds HB, salt bridge, C–H···π and π–π stacking, **1**–**5** in Figure 1B) played a role.[20] Taking into consideration a need for novel biodetoxifying agents and dual-cavity $\mathbf{1}^{6-}$ capable of sequestering doxorubicin in

[a] *Department of Chemistry & Biochemistry, The Ohio State University, 100 West 18th Avenue, 43210 Columbus, Ohio (USA).*
Electronic Supplementary Information (ESI) available: [Experimental details, additional spectroscopic and computational results]. See DOI: 10.1039/x0xx00000x

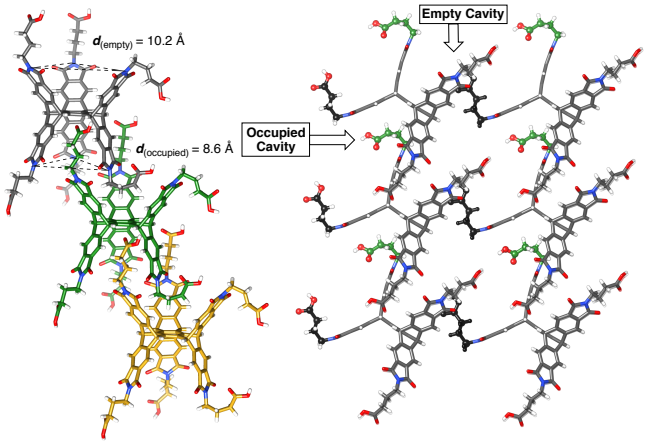

Figure 2. Two views of the solid-state structure of **1** depict dual-cavity baskets, each with two of their γ-aminobutyric acids (green and black) fastening the three three-dimensional network of hosts.

the form of stable nanoparticles, we envisioned a possibility of our hosts acting as cooperative[21] nano-antidotes.[3] Correspondingly, we wondered if there was a way to direct the allosteric complexation of targeted drugs (and toxicants)[22] for triggering their sequestration within a narrow range of concentrations?[23] Moreover, are there any requirements in terms of size and electronic characteristics of guests to bind to $\mathbf{1}^{6-}$?[24] To answer these questions, we investigated the binding modes (i.e. allostery) and affinity of $\mathbf{1}^{6-}$ toward a series of differently sized and functionalized aromatics of which most are being used as anticancer therapeutics (Figures 1C and 4A).[25]

A slow diffusion of dichloromethane/heptane to a solution of **1** in DMSO led to the formation of single crystals. After subjecting the sample to diffraction analysis, we found two molecules of **1** populating the unit cell with somewhat disordered γ-aminobutyric acid groups at their termini (see SI). In the solid state, baskets assembled into linear supramolecular polymers (Figure 2, left) with each host placing one of its aliphatic arms in the inner space of its neighbour. Concurrently, γ-Aminobutyric acid from the adjoined phthalimide (Figure 2, right) reached to another column of baskets to reside in the proximity of the empty cavity of **1**. For all molecules of **1**, the pocket occupied with the aliphatic chain contracted ($d_{(occupied)}$ = 8.6 Å, Figure 2) while the empty one expanded ($d_{(empty)}$ = 10.2 Å, Figure 2). Such induced-fit mode of recognition[19] in the solid state was expected to play a role in the allosteric encapsulation in solution, as discussed below.[15a]

An incremental addition of a standard solution of dimethyl phenylphosphonate (DMPP, **2**; Figure 1C) to $\mathbf{1}^{6-}$ (10 mM PBS buffer at pH = 7.0) was monitored with ^{1}H NMR spectroscopy (Figure S1). A steady perturbation of chemical shifts of resonances from both compounds suggested that the complexation was occurring fast on the NMR time scale. The binding isotherm fit well to the model corresponding the formation of binary [$\mathbf{2}\subset\mathbf{1}^{6-}$] with $K_1 = 2.6 \pm 1.1 \cdot 10^3$ M^{-1} (Figure S2).[26] On the basis of a greater magnitude of diamagnetic shielding of aromatic resonances in **2** (Figure S3), we deduced that the OP guest docked in the basket's cavity by using its benzene ring (Figure 1C);[27] ^{1}H-^{1}H NOESY correlations supported such complexation geometry (Figure S4). In a similar manner, the inclusion of somewhat larger naproxen $\mathbf{3}^-$ (200 Å^2, Figure 1C) occurred with the formation of binary [$\mathbf{3}^-\subset\mathbf{1}^{6-}$] with the methoxy portion of the naphthalene's ring entering the host's aromatic cavity (Figures S5/S6). Interestingly, the thermodynamic stability of [$\mathbf{3}^-\subset\mathbf{1}^{6-}$] ($K_1 = 0.48 \pm 0.14 \cdot 10^3$ M^{-1}; Figure S7) was similar to [$\mathbf{2}\subset\mathbf{1}^{6-}$] with the naproxen's negative charge presumably curtailing the association.[28] Monitoring the complexation of similarly sized proflavine $\mathbf{4}^+$ (202 Å^2, Figure 1C), however, resulted in resonances from the antiseptic agent broadening into the baseline (Figure S8). On the other hand, the signals from host $\mathbf{1}^{6-}$ underwent small yet gradual shifts. The inclusion and immobilization of positively charged proflavine (Figure 1C) was likely to increase the relaxation time of its protons and thus contribute broadening the apparent linewidth of the resonances.[29] With the stability of the complex being large and therefore unsuitable to study with ^{1}H NMR spectroscopy (Figure S8) we turned to fluorescence spectroscopy.[14] An incremental addition of $\mathbf{1}^{6-}$ to a standard solution of $\mathbf{4}^+$ led to the quenching of the drug's emission (Figure S9). The binding isotherm fit well to the formation of binary [$\mathbf{4}^+\subset\mathbf{1}^{6-}$] with $K_1 = 1.12 \pm 0.02 \cdot 10^5$ M^{-1} (Figure S10). Following, we used fluorescence (Figures S14/S17) to examine

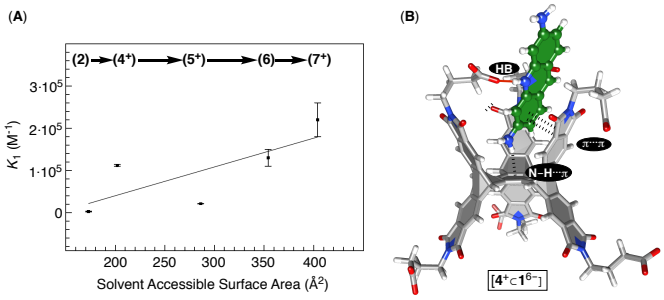

Figure 3. (A) A plot showing experimentally determined association constants K_1 (M^{-1}) corresponding to the formation of binary [$\mathbf{2}$–$\mathbf{7}^+\subset\mathbf{1}^{6-}$] as a function of guest's solvent-accessible surface area (PM3, Spartan). The data were fit to a linear function (R^2 = 0.6) using SigmaPlot13. (B) Energy-minimized (MM/MC, OPLS3) and most stable conformers of [$\mathbf{4}^+\subset\mathbf{1}^{6-}$] showing a single carboxylate arm reaching to proflavine and forming a charged HB while the bottom portion of the guest engages in N–H···π and π ···π interactions.

the complexation of increasingly larger topotecan $\mathbf{5}^+$ (286 Å^2, Figure 1C),[14] RhB **6** (354 Å^2, Figure 1C) and irinotecan $\mathbf{7}^+$ (404 Å^2, Figure 1C). The nonlinear least-square analyses of binding isotherms[26] were for all three guests in line with the formation of binary complexes (Figures S15/S18), possessing nearly μM stabilities (Figure 3A). At last, the results of ^{1}H NMR supramolecular titrations (Figures S11–S13/S16) provided evidence suggesting that $\mathbf{5}^+$–$\mathbf{7}^+$ occupied the aromatic cavity of $\mathbf{1}^{6-}$ using their lactone or xanthene rings (Figure 1C).

When the solvent-accessible surface area (Spartan, PM3; Figure 1C) of neutral or positively charged $\mathbf{2}$–$\mathbf{7}^+$ were plotted against the measured stabilities (K_1) of [$\mathbf{2}$–$\mathbf{7}^+\subset\mathbf{1}^{6-}$], there appeared a somewhat linear trend (Figure 3A); since naproxen $\mathbf{3}^-$ carried negative charge (see its EPS in Figure 1C), we excluded it from consideration.[30] With increasingly larger nonpolar surfaces imparting a more effective complexation, we concluded that the hydrophobic effect[31] played the principal

role in the association of these guests. That is to say, desolvation of both $\mathbf{1}^{6-}$ and $\mathbf{2}$–$\mathbf{7}^{+}$ was in polar water progressively more effective to dominate the process. In fact, three carboxylates at the periphery of $\mathbf{1}^{6-}$ could form favourable contacts with positive sites in each guest (see their EPS in Figure 1C): computational results (MM, OPLS3) showed single or no CO_2^- groups participating (Figure 3B, see SI). It follows that the formation of binary complexes [$\mathbf{2}$–$\mathbf{7}^{+}\subset\mathbf{1}^{6-}$] and the apparent negative allostery (K_1>>K_2 and α < 1) could be arising from the paucity of directional host-guest contacts.[20] These contacts are thought to be necessary to compensate (but also assist) the induced-fit mode of complexation (Figure 2) in which two conjoined cavitands ought to undergo conformational adjustments[15a] to accommodate their guests.[14] The results of DLS (Figures S19-S22) and TEM measurements showed that all complexes [$\mathbf{2}$–$\mathbf{7}^{+}\subset\mathbf{1}^{6-}$] assembled into spherical nanoparticles (c.a. 50 nm, Figures S23-27).

Anthracyclines $\mathbf{8}^{+}$–$\mathbf{11}^{+}$ are clinically useful anticancer agents[32] that operate by intercalating[33] into DNA, bound to topoisomerase II, to inhibit the enzyme decatenating interlocked rings of nucleic acids during the process of replication.[34] Interestingly, these positively charged drugs would also partition and accumulate into negatively charged cardiolipin (phospholipid), which is believed to cause cardiotoxicity[35] and various heart disfunctions.[36] In this regard, sufficiently large (355 Å^2) and anionic $\mathbf{1}^{6-}$ was found[14] to complex two cationic doxorubicin $\mathbf{8}^{+}$ in the allosteric manner with $\alpha = 4K_2/K_1 = 1.1 \pm 0.3 \cdot 10^2$. By intercalating in the basket's aromatic cavities (C–H···π **1** and π–π stacking **2**, Figure 4A), we hypothesized that each guest positioned its aminosugar against carboxylate appendages to establish two HBs (**3** and **5**, Figure 4A) and a salt bridge (**4**, Figure 4A). In consequence, we hereby reasoned that the removal of favourable noncovalent contacts **1**–**5** should have an effect on the complexation and, perhaps, allostery. Accordingly, we decided to probe the encapsulation of daunorubicin $\mathbf{9}^{+}$, idarubicin $\mathbf{10}^{+}$ and epirubicin $\mathbf{11}^{+}$ (Figure 4A), all with the anthraquinone core but (a) lacking the key 14-hydroxyl and 4-methoxy groups or (b) possessing 4'-OH on the aminosugar in the equatorial instead of axial position. First, an incremental addition of $\mathbf{9}^{+}$–$\mathbf{11}^{+}$ to the standard solution of $\mathbf{1}^{6-}$ showed ^{1}H NMR spectroscopic changes (Figures S28/S31/S34) similar to those recorded for doxorubicin $\mathbf{8}^{+}$.[14] That is to say, a broadening of aromatic signals into the baseline with a less dramatic perturbation of resonances from the aliphatic portion of anticancer drugs $\mathbf{9}^{+}$–$\mathbf{11}^{+}$ suggested for their mode of docking to be similar to $\mathbf{8}^{+}$ (Figure 4A). Second, we quantified the complexations by monitoring the fluorescence quenching of anthracyclines $\mathbf{9}^{+}$–$\mathbf{11}^{+}$ upon the addition of basket $\mathbf{1}^{6-}$ to their aqueous solution (Figures S29/S32/S35). The binding isotherms would, in each case (Figures S30/S33/S36), fit well to the model describing a consecutive formation of binary and ternary complexes characterized with binding constants K_1 and K_2 (Figure 4B).[26] From the plot depicting the values of K_1 along the series, we noted comparably weaker affinity of $\mathbf{9}^{+}$–$\mathbf{11}^{+}$ than $\mathbf{8}^{+}$ toward $\mathbf{1}^{6-}$. That is to say, the stability of binary [$\mathbf{9}^{+}$–$\mathbf{11}^{+}\subset\mathbf{1}^{6-}$] was, on average, 0.7 ± 0.2 kcal/mol lower ($\Delta\Delta G^\circ_1$, Figure 4B) than [$\mathbf{8}^{+}\subset\mathbf{1}^{6-}$]. Since this value is within 0.3–1.8 kcal/mol corresponding to the strength of uncharged HBs of proteins in water,[37] the result provided support to the notion that terminal carboxylates engaged in hydrogen bonding with functional groups from the drugs (Figure 4A). On the contrary, the second binding K_2 was greater in the case of [($\mathbf{9}^{+}$–$\mathbf{11}^{+}$)$_2\subset\mathbf{1}^{6-}$]] than [$\mathbf{8}^{+}\subset\mathbf{1}^{6-}$] with $\Delta\Delta G^\circ_2 = 0.5 \pm 0.1$ kcal/mol (Figure 4B). As a result of the apparent K_1/K_2 compensation, thermodynamic stabilities of [($\mathbf{8}^{+}$–$\mathbf{11}^{+}$)$_2\subset\mathbf{1}^{6-}$] and [$\mathbf{9}_2^{2+}\subset\mathbf{1}^{6-}$] were almost identical ($K_1 \cdot K_2$ = 10^{12} M^{-1}). The less favourable

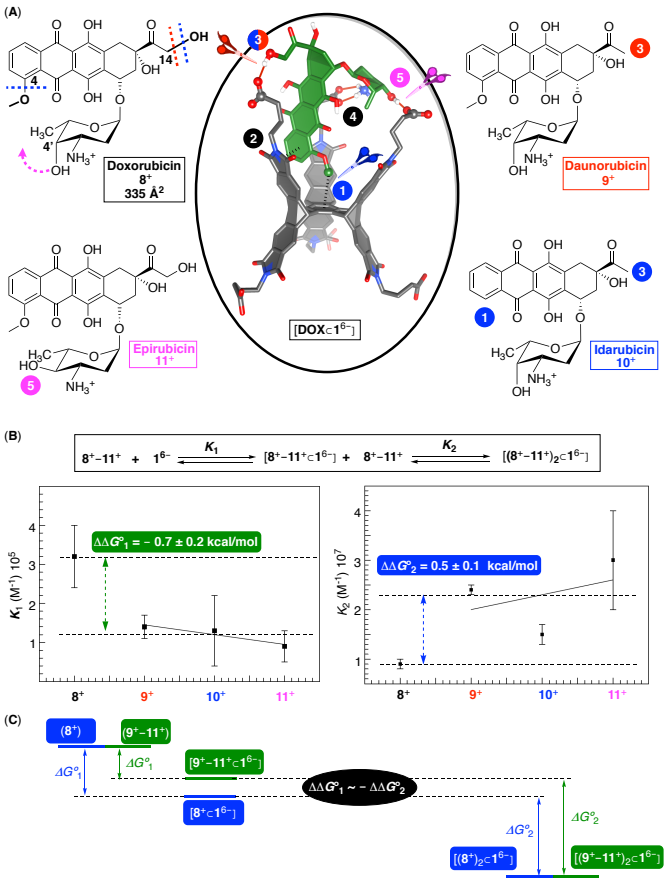

Figure 4. (A) Chemical structures of anthracyclines $\mathbf{8}^{+}$–$\mathbf{11}^{+}$ with energy-minimized (MM, OPLS3) structure of [$\mathbf{8}^{+}\subset\mathbf{1}^{6-}$] showing five (**1**–**5**) noncovalent and coloured host-guest contacts. (B) Plots showing binding constants K_1 (left) and K_2 (right) corresponding to the formation of [$\mathbf{8}^{+}$–$\mathbf{11}^{+}\subset\mathbf{1}^{6-}$] and [($\mathbf{8}^{+}$–$\mathbf{11}^{+}$)$_2\subset\mathbf{1}^{6-}$] determined with fluorescence supramolecular titrations. Free energies $\Delta\Delta G^\circ_1$ and $\Delta\Delta G^\circ_2$ were obtained as $\Delta G^\circ_1(\mathbf{8}^{+}) - (\Delta G^\circ_1(\mathbf{9}^{+}) + \Delta G^\circ_1(\mathbf{10}^{+}) + \Delta G^\circ_1(\mathbf{11}^{+}))/3$ and $\Delta G^\circ_2(\mathbf{8}^{+}) - (\Delta G^\circ_2(\mathbf{9}^{+}) + \Delta G^\circ_2(\mathbf{10}^{+}) + \Delta G^\circ_2(\mathbf{11}^{+}))/3$, respectively. (C) A graphical representation of the complexation event and the corresponding free energies; note that green $\Delta G^\circ_1 = (\Delta G^\circ_1(\mathbf{9}^{+}) + \Delta G^\circ_1(\mathbf{10}^{+}) + \Delta G^\circ_1(\mathbf{11}^{+}))/3$ and $\Delta G^\circ_2 = (\Delta G^\circ_2(\mathbf{9}^{+}) + \Delta G^\circ_2(\mathbf{10}^{+}) + \Delta G^\circ_2(\mathbf{11}^{+}))/3$.

assembly of $\mathbf{9}^{+}$–$\mathbf{11}^{+}$ and $\mathbf{1}^{6-}$ into [$\mathbf{9}^{+}$–$\mathbf{11}^{+}\subset\mathbf{1}^{6-}$] ($\Delta\Delta G^\circ_1$ = – 0.7 kcal/mol) though enabled a more favourable formation of [($\mathbf{9}^{+}$–$\mathbf{11}^{+}$)$_2\subset\mathbf{1}^{6-}$]] ($\Delta\Delta G^\circ_2$ = 0.5 kcal/mol, Figure 4C). In one scenario,[15a] the "looser" basket-guest contacts provided additional flexibility for completing conformational changes necessary to accommodate another guest without causing much strain. A curious outcome of the observed compensation is greater positive allostery (α) characterizing the formation of [($\mathbf{9}^{+}$–$\mathbf{11}^{+}$)$_2\subset\mathbf{1}^{6-}$] ($\alpha_{(mean)} = 8 \pm 3 \cdot 10^2$) than [($\mathbf{8}^{+}$)$_2\subset\mathbf{1}^{6-}$] ($\alpha = 1.1 \pm 0.3 \cdot 10^2$); $\alpha(\mathbf{9}^{+}$–$\mathbf{11}^{+})/\alpha(\mathbf{8}^{+}) = 7 \pm 3$, which is equivalent to 1.2 kcal/mol (Figure 4C). Evidently, weakening the stability of binary complexes would, in the case at hand, lead to a more effective

capture of the second guest and greater homotropic cooperativity.[21] Finally, all four complexes [(**8**$^{+}$**–11**$^{+}$)$_2$⊂**1**$^{6-}$] assembled into spherical nanoparticles (circa 50 nm, Figures S37–S42).

To sum up, dual-cavity baskets carrying six γ-aminobutyric acids at top of their two conjoined cavities trap differently sized aromatics with binary and/or ternary complexes assembling into spherical nanoparticles in PBS. The greater the surface area of the guests the more effective the encapsulation with the hydrophobic effect driving the process.[38] In terms of the complexation of anthracyclines, the synergy between hydrophobic effect and host-guest hydrogen bonding permitted the allosteric formation of stable ternary assemblies.[20] Weakening the first complexation (i.e. by removing HB contact(s)), made the second one stronger with the compensation enhancing the homotropic cooperativity. Our findings should be useful for creating allosteric nano-antidotes capable of rapid, selective and effective removal of toxic compounds from biological systems, necessitating additional *in vitro/vivo* cell studies about which we aim to report in the future.

Conflicts of interest

There are no conflicts to declare.

Acknowledgement

This work was financially supported with funds obtained from ARO (W911NF-17-1-0140). Generous computational resources from the OSC are gratefully acknowledged.

References

1. L. Zhang and J.-C. Leroux, *Adv. Drug Delivery Rev.*, 2015, **90**, 1-2.
2. L. C. Smith, P. T. Bremer, C. S. Hwang, B. Zhou, B. Ellis, M. S. Hixon and K. D. Janda, *J. Am. Chem. Soc.*, 2019, **141**, 10489-10503.
3. V. Forster and J.-C. Leroux, *Sci. Transl. Med.*, 2015, **7**, 1-8.
4. A. Damalas Christos and D. Koutroubas Spyridon, *Toxics*, 2016, **4**.
5. (a) J.-C. Leroux, *Nat. Nanotechnol.*, 2007, **2**, 679-684; (b) L. M. Graham, T. M. Nguyen and S. B. Lee, *Nanomedicine*, 2011, **6**, 921-928.
6. (a) A. J. Kassick, H. N. Allen, S. S. Yerneni, F. Pary, M. Kovaliov, C. Cheng, M. Pravetoni, N. D. Tomycz, D. M. Whiting, T. L. Nelson, M. Feasel, P. G. Campbell, B. Kolber and S. Averick, *ACS Appl. Bio Mater.*, 2019, **2**, 3418-3428; (b) Anon, *Nat. Med.,* 2013, **19**, 1194-1195.
7. S. Rojas, T. Baati, L. Njim, L. Manchego, F. Neffati, N. Abdeljelil, S. Saguem, C. Serre, M. F. Najjar, A. Zakhama and P. Horcajada, *J. Am. Chem. Soc.*, 2018, **140**, 9581-9586.
8. F. Zheng and C.-G. Zhan, *Future Med. Chem.*, 2012, **4**, 125-128.
9. F. Zheng, L. Xue, S. Hou, J. Liu, M. Zhan, W. Yang and C.-G. Zhan, *Nat. Commun.*, 2014, **5**, 4457-4458.
10. P. T. Bremer, A. Kimishima, J. E. Schlosburg, B. Zhou, K. C. Collins and K. D. Janda, *Angew. Chem., Int. Ed.*, 2016, **55**, 3772-3775.
11. (a) S. Ganapati, S. D. Grabitz, S. Murkli, F. Scheffenbichler, M. I. Rudolph, P. Y. Zavalij, M. Eikermann and L. Isaacs, *ChemBioChem*, 2017, **18**, 1583-1588; (b) R. A. Tromans, T. S. Carter, L. Chabanne, M. P. Crump, H. Li, J. V. Matlock, M. G. Orchard and A. P. Davis, *Nat. Chem.*, 2019, **11**, 52-56.
12. A. Bom, M. Bradley, K. Cameron, J. K. Clark, J. Van Egmond, H. Feilden, E. J. MacLean, A. W. Muir, R. Palin, D. C. Rees and M.-Q. Zhang, *Angew. Chem., Int. Ed.*, 2002, **41**, 265-270.
13. F. Haerter, J. C. P. Simons, U. Foerster, I. Moreno Duarte, D. Diaz-Gil, S. Ganapati, K. Eikermann-Haerter, C. Ayata, B. Zhang, M. Blobner, L. Isaacs and M. Eikermann, *Anesthesiology*, 2015, **123**, 1337-1349.
14. W. Wang, H. Wang, L. Zhiquan, H. Xie, H. Cui and J. D. Badjic, *Chem. Sci.*, 2019, **10**, 5678-5685.
15. (a) S. Chen, M. Yamasaki, S. Polen, J. Gallucci, C. M. Hadad and J. D. Badjic, *J. Am. Chem. Soc.*, 2015, **137**, 12276-12281; (b) S. Shinkai, M. Ikeda, A. Sugasaki and M. Takeuchi, *Acc. Chem. Res.*, 2001, **34**, 494-503.
16. G. Ercolani, *J. Am. Chem. Soc.*, 2003, **125**, 16097-16103.
17. S. E. Border, R. Z. Pavlovic, Z. Lei, M. J. Gunther, H. Wang, H. Cui and J. D. Badjic, *Chem. Commun.*, 2019, **55**, 1989.
18. A. Hunter Christopher and L. Anderson Harry, *Angew. Chem. Int Ed Engl*, 2009, **48**, 7488-7499.
19. L. Zhiquan, H. Xie, S. E. Border, J. Gallucci, R. Z. Pavlovic and J. D. Badjic, *J. Am. Chem. Soc.*, 2018, **140**, 11091-11100.
20. H. Yao, H. Ke, X. Zhang, S.-J. Pan, M.-S. Li, L.-P. Yang, G. Schreckenbach and W. Jiang, *J. Am. Chem. Soc.*, 2018, **140**, 13466-13477.
21. Y. Li, Y. Wang, G. Huang and J. Gao, *Chem. Rev.*, 2018, **118**, 5359-5391.
22. H. J. Oh, M. S. Aboian, M. Y. J. Yi, J. A. Maslyn, W. S. Loo, X. Jiang, D. Y. Parkinson, M. W. Wilson, T. Moore, C. R. Yee, G. R. Robbins, F. M. Barth, J. M. DeSimone, S. W. Hetts and N. P. Balsara, *ACS Cent. Sci.*, 2019, **5**, 419-427.
23. (a) J. S. Park, F. Le Derf, C. M. Bejger, V. M. Lynch, J. L. Sessler, K. A. Nielsen, C. Johnsen and J. O. Jeppesen, *Chem. - Eur. J.*, 2010, **16**, 848-854; (b) J. A. Riddle, X. Jiang, J. Huffman and D. Lee, *Angew. Chem., Int. Ed.*, 2007, **46**, 7019-7022; (c) I. Saha, J. H. Lee, H. Hwang, T. S. Kim and C.-H. Lee, *Chem. Commun.*, 2015, **51**, 5679-5682.
24. S. Chen, L. Wang, S. M. Polen and J. D. Badjic, *Chem. Mater.*, 2016, **28**, 8128-8131.
25. A. Todd, P. W. Groundwater and J. H. Gill, *Anticancer therapeutics: from drug discovery to clinical applications*, 2018.
26. P. Thordarson, *Chem. Soc. Rev.*, 2011, **40**, 1305-1323.
27. S. E. Border, R. Z. Pavlovic, L. Zhiquan and J. D. Badjic, *J. Am. Chem. Soc.*, 2017, **139**, 18496-18499.
28. H. Xie, L. Zhiquan, R. Z. Pavlovic, J. Gallucci and J. D. Badjic, *Chem. Commun.*, 2019, **55**, 5479-5482.
29. S. Chen, Y. Ruan, J. D. Brown, J. Gallucci, V. Maslak, C. M. Hadad and J. D. Badjic, *J. Am. Chem. Soc.*, 2013, **135**, 14964-14967.
30. L. Zhiquan, S. M. Polen, C. M. Hadad, T. V. RajanBabu and J. D. Badjic, *Org. Lett.*, 2017, **19**, 4932-4935.
31. H.-J. Schneider, *Angew. Chem., Int. Ed.*, 2009, **48**, 3924-3977.
32. S. Zhu, L. Yan, X. Ji and W. Lu, *J. Mol. Struct. THEOCHEM*, 2010, **951**, 60-68.
33. A. Rescifina, C. Zagni, M. G. Varrica, V. Pistara and A. Corsaro, *Eur. J. Med. Chem.*, 2014, **74**, 95-115.
34. F. Yang, S. S. Teves, C. J. Kemp and S. Henikoff, *Biochim. Biophys. Acta, Rev. Cancer*, 2014, **1845**, 84-89.
35. B. E. Levis, P. F. Binkley and C. L. Shapiro, *Lancet Oncol.*, 2017, **18**, e445-e456.
36. F. d. S. Arruda, F. D. Tome, M. P. Miguel, L. Borges de Menezes, P. R. Alo Nagib, E. C. Campos, D. F. Soave and M. R. N. Celes, *Curr. Pharm. Des.*, 2019, **25**, 109-118.
37. C. N. Pace, *Nat. Struct. Mol. Biol.*, 2009, **16**, 681-682.
38. W. Liu, A. Johnson and B. D. Smith, *J. Am. Chem. Soc.*, 2018, **140**, 3361-3370.

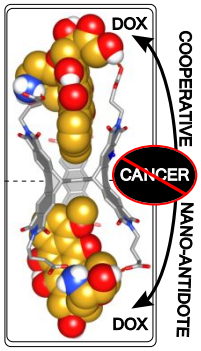

Dual-cavity baskets, carrying six γ-aminobutyric acids, sequester anticancer anthracyclines in the cooperative manner, to be of interest for creating nano-antidotes.